Pergamon

Spectrochimica Acta, Vol. 51A, No. 1, pp. 1–9, 1995
Elsevier Science Ltd. Printed in Great Britain
0584–8539/95 $9.50 + 0.00

0584–8539(94)E0084–N

Fourier-transform infrared/photoacoustic study of pyridine adsorbed on silica supported copper–molybdenum catalysts

MOHAMED MOKHTAR MOHAMED

Al-Azhar University, Faculty of Science, Chemistry Department, Nasser City, Cairo, Egypt

(*Received* 28 *October* 1993; *in final form* 20 *February* 1994; *accepted* 22 *February* 1994)

Abstract—Pyridine adsorption is used to study the acidic sites of silica-supported $CuO–MoO_3$ catalysts, with reference to CuO/SiO_2 and MoO_3/SiO_2 catalysts. At low wt% of copper, both Lewis and Bronsted acid sites are present on the $CuO–MoO_3/SiO_2$ surface. A substantial decrease and then vanishing of the Bronsted acidity is obtained as a result of increasing the copper loading. An approach confining the prevalence of Lewis acidity over the Bronsted ones is described and discussed. A new band of Lewis acidity is observed at 1574 cm^{-1} and attributed to the presence of $CuMoO_4$ species. This band is not observed in the individual oxide form of both CuO/SiO_2 and MoO_3/SiO_2 catalysts. Carbon monoxide adsorption on $CuO–MoO_3/SiO_2$ catalysts reflects a major dispersion if it is compared with CuO/SiO_2 and MoO_3/SiO_2 catalysts and also gives a picture about the expected structures of these supported oxide catalysts. Copper is found also to exert a major control on the mode of interaction of molybdenum species with the silica surface. Moreover, important correlations and shifts in the IR bands are evaluated and discussed.

INTRODUCTION

IN VIEW of the industrial importance of catalysts consisting of molybdenum supported on silica with promoters such as Co or Ni, considerable attention has been paid to understand the effect of the support, the form in which molybdenum and the promoter atom are present and their role in the reaction [1–3].

A great deal of effort has been devoted to demonstrate the deactivation, thermal stability and different acid centres originated on the above-mentioned bimetallic catalysts, Mo–Co and Mo–Ni, supported on alumina [4–6].

Very little work seems to have been done on the effect of copper (as a promoter) on the activity of MoO_3/SiO_2 catalysts. A Fourier-transform infrared/photoacoustic (FTIR/PA) study has been carried out, in the low frequency vibrations as well as in the hydroxyl group region [7], to examine the influence of copper loading on the Mo–silica catalysts. However, detailed information about the metallic sites, enhancement of the reducibility of the molybdenum ions in $CuO–MoO_3/SiO_2$ catalysts is investigated and discussed.

Copper–molybdenum oxide catalysts supported on silicon oxide will show definitely another type of acidic centre different from those of copper–molybdenum catalysts, used in oxidative dehydrogenation of butene-1, giving butadiene and carbon monoxide [8] as main products. Therefore, the catalytic performance of $Cu–Mo/SiO_2$ samples will be the next goal for improving the catalytic activity of the dehydrogenation reaction of butene-1, after establishing the acidity of the catalyst and demonstrating the unique promotor interactions in the $Cu–Mo/SiO_2$ catalysts.

A FTIR/PA technique is used for recording the IR spectra of the samples. A detailed discussion of the effects of both copper loading and thermal treatment on the molybdenum–silica acidity is presented and discussed.

EXPERIMENTAL

Silica gel60 (Merck) is used as a support. The silica gel is thermally pretreated for 17 h in vacuum up to 673 K and showed a surface area of 456 $m^2 g^{-1}$, maximum incremental pore volume of 0.1023 $cm^3 g^{-1}$ and maximum incremental pore area of 88.08 $m^2 g^{-1}$.

The Cu–Mo catalysts are prepared by consecutive deposition of molybdenum and copper atoms respectively onto the silica support. First, the 9wt MoO_3/SiO_2 catalyst is prepared by a wet impregnation method with ammonium heptamolybdate. Further procedural details can be found elsewhere [9].

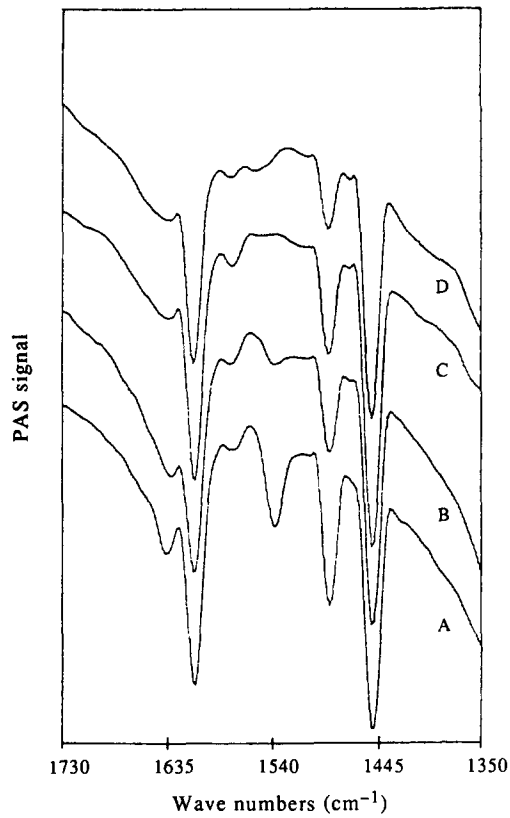

Fig. 1. FTIR/PA spectra of pyridine adsorbed, at 393 K, on oxidized catalysts supported on silica gel60: (A) 1wt% CuO–9wt% MoO_3; (B) 3wt% CuO–9wt% MoO_3; (C) 6.6wt% CuO–9wt% MoO_3; (D) 15wt% CuO–9wt% MoO_3.

The *x*wt% Cu–9wt% Mo/SiO_2 samples are prepared by the addition of copper nitrate solutions onto the 9wt% Mo/SiO_2 catalyst. Excess water is evaporated (343–353 K), dried (383 K), heated in air (3 h, 648 K) and calcined (6 h, 773 K).

The supported oxide *x*wt% Cu–9wt% Mo/SiO_2 catalysts, designated as 1wt% Cu–9wt% Mo, 3wt% Cu–9wt% Mo, 6.6wt% Cu–9wt% Mo, 9wt% Cu–9wt% Mo and 15wt% Cu–9wt% Mo, are subjected to pyridine adsorption in a dynamic, volumetric sorption apparatus, made of glass. More details about the apparatus can be found elsewhere [10].

The sample is heated in vacuum (10^{-3} Torr) to 723 K (5°C min^{-1}) for 4 h before pyridine adsorption takes place, *in situ*, at 393 K. Pyridine adsorption is admitted, at its saturation vapour pressure, on the sample for 2 h and evacuated at the same temperature (393 K) for 0.5 h.

Adsorption of CO on the catalyst samples is recorded at room temperature. The samples are placed in a dry nitrogen purged-glovebox before recording the IR measurements. Under these dry conditions, the sample is loaded in the photoacoustic cell.

The PA spectra are recorded, at room temperature, on a Nicolet 5-DXB-FTIR-spectrometer. The PA cell MTEC-100, which is purged with He gas, is connected to a very sensitive (50 mV Pa^{-1}) Burel–Kjaer microphone.

The sample cup is made from stainless steel with a diameter of 6 mm and a depth of 3 mm. An average of 500 scans is used for the transformation and the mirror velocity is 0.08 cm s^{-1}.

The spectra presented in this study are taken at 4 cm^{-1} resolution.

RESULTS AND DISCUSSION

Infrared spectroscopy of adsorbed pyridine is used to determine the different acid sites and to probe the acid strength of those sites.

The absorption spectra of pyridine adsorbed on the oxidized *x*wt% Cu–9wt% Mo/SiO_2 catalysts, evacuated at 393 K, where *x* represents 1, 3, 6.6 and 15wt% Cu loading, respectively, are shown in Fig. 1.

There are six major bands for 1wt% Cu–9wt% Mo/SiO_2 sample at 1450, 1487, 1574, 1608, 1538 and 1636 cm^{-1}. These correspond to the 19b, 19a, 8b, 8a, 8b and 8a bands of pyridine adsorbed on Lewis acid sites (19b, 19a, 8b and 8a) and on Bronsted acid sites (8b and 8a), respectively.

As the copper loading is increased, major changes in the bands occur. The disappearance of the 8b band at 1537 cm^{-1} is accomplished starting from 6.6wt% of copper. Whereas the 8a band at 1636 cm^{-1} is significantly decreased and shows a shift to a lower wave number, 1632 cm^{-1}, upon increasing the wt% of copper. It is of interest to note also the significant increase of Lewis acidity over the Bronsted acidity for 8b and 8a bands upon increasing the copper content.

Furthermore, the strong band at 1487 cm^{-1}, which represents both Lewis and Bronsted acidity [11], observed in both CuO/SiO_2 and MoO_3/SiO_2 catalysts, shows a significant decrease as a result of increasing the copper loading.

Figure 2 shows the IR spectra of pyridine adsorbed, at 393 K, on 9wt% CuO/SiO_2, 9wt% MoO_3/SiO_2 and 9wt% CuO–9wt% MoO_3/SiO_2 catalysts.

Spectrum A of 9wt% CuO/SiO_2 catalyst, shows the 19b band at 1450 cm^{-1}, of a Lewis site, and the 8a band at 612 cm^{-1} along with a small band at 1488 cm^{-1} [12].

Spectrum B of 9wt% MoO_3/SiO_2 catalyst, generates both Lewis and Bronsted acid sites. The bands at 1635 and 1532 cm^{-1} are assigned to pyridine adsorbed on Bronsted acid sites [13, 14]. The other bands in the spectrum (1608 and 1450 cm^{-1}) are assigned to pyridine adsorbed on Lewis acid sites except the 1485 cm^{-1} band which represents the contribution of both sites together.

It is obvious that the intensity of the bands (either Lewis or Bronsted) in the 9wt% MoO_3 sample exceeds that of the 9wt% CuO sample. This reflects the enhancement of acid sites for Mo–silica compared with Cu–silica.

This increase in total acidity is caused primarily by the increase in Bronsted acidity, resulting from the presence of molybdena as clusters and layered oxides [15, 16].

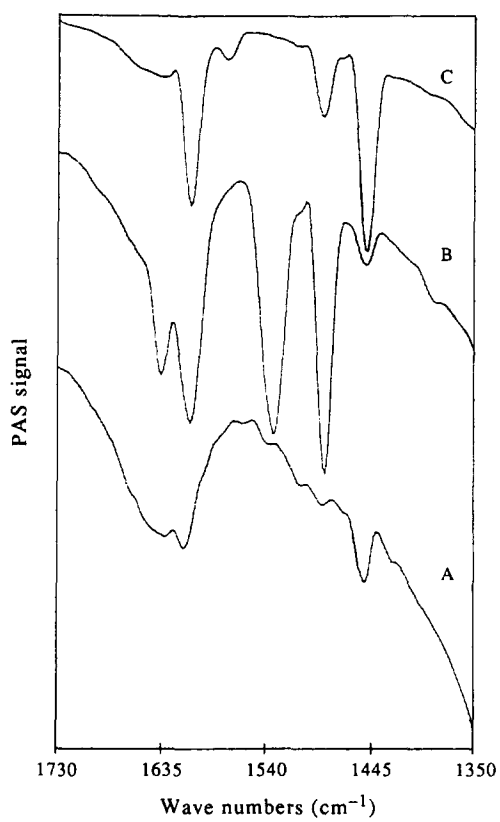

Fig. 2. FTIR/PA spectra of pyridine adsorbed, at 393 K, on the following catalysts supported on silica gel60: (A) 9wt% CuO/SiO_2; (B) 9wt% MoO_3/SiO_2; (C) 9wt% CuO–9wt% MoO_3/SiO_2.

It should be noted also that the 1450 cm^{-1} band intensity (Figs 2(A) and (B)) is more important on Cu–silica relative to Mo–silica and the strength of Lewis sites on Cu–silica is much higher than those on Mo–silica since the former is characterized by a band at 1612 cm^{-1} whereas the latter at 1608 cm^{-1}.

Spectrum C of 9wt% CuO–9wt% MoO_3/SiO_2 sample, shows bands at 1450, 1488, 1574 and 1608 cm^{-1}. This spectrum reflects a new band at 1574 cm^{-1} (8b) of Lewis acidity and the disappearance of 1635 and 1532 cm^{-1} bands of Bronsted acid sites. The band at 1488 cm^{-1} decreases in intensity and shifts to longer wave number compared with the individual supported oxide catalyst. Furthermore, an extensive increase in intensity of the 1450 cm^{-1} band is observed.

As is evident from this spectrum, an increase in the number and strength of Lewis acid sites while a decrease of Bronsted acid sites is observed.

This can be explained by KATAOKA and DUMESIC [17] who stated that the terminal double bonded oxygens for molybdena are essential for creating Bronsted acid sites. However, any distortion in this environment will induce a great loss in Bronsted acidity. This distortion has been obtained as a result of the involvement of copper atoms in the Mo–silica structure.

More information can be obtained through the comparison of CuO/SiO_2 and MoO_3/SiO_2 against Cu–Mo/SiO_3 catalysts.

The 1532 cm^{-1} (8b) band, in the MoO_3/SiO_2 catalyst, is shifted to 1537 cm^{-1}, in the 1wt% Cu–9wt% Mo/SiO_2 catalyst, indicating the strength of Bronsted acidity at such low wt% of copper.

On the contrary, the 1636 cm^{-1} band, of 8a type, observed in the 1wt% Cu–9wt% Mo/SiO_2 catalyst is shifted to 1632 cm^{-1} in the 3wt% Cu–9wt% Mo/SiO_2 catalyst showing a decrease in Bronsted acidity of that site upon increasing the copper loading.

The 1537 cm^{-1} band, which is the most characteristic of Bronsted acidity, is only observed at low loading of copper (1 and 3wt% Cu–9wt% Mo). This could clarify the predominancy of Lewis acidity over the Bronsted acidity in a stepwise manner connected with the successive addition of copper content. It is of interest also to notice the consistancy of the strong band at 1450 cm^{-1} in Figs 1(A) and 2(C). This is a consequence of the blocking of the small pores, in silica, at such high wt% of molybdenum which implies very small decrease in the integrated area under the peak. Therefore, most probably pyridine is adsorbed on the surface and not inside the pores. Site heterogeneity might be another plausible explanation for the constant behaviour of the 1450 cm^{-1} band.

These results suggest that there is a detachment of the molybdenum species from the SiO_2 support as a result of increasing the copper loading and this imparts the formation of $CuMoO_4$ species. Similar results for the $CoMoO_4$ formation are obtained [18].Therefore, it is likely to attribute the 1574 cm^{-1} band of Lewis acidity to the copper–molybdate species.

Since MOHAMED *et al.* [7] assigned an IR frequency observed at 923 cm^{-1}, in 3–15wt% Cu–9wt% Mo/SiO_2 catalysts, to the presence of $CuMoO_4$ species as a result of the disappearance of any observed band for the individual oxide form, of both Mo and Cu supported on silica, in the 910–930 cm^{-1} range.

Infrared spectra of pyridine desorbed from the oxidized 9wt% Cu–9wt% Mo/SiO_2 catalysts, at different evacuation temperatures, are shown in Fig. 3 and the absorption frequencies are tabulated in Table 1.

There are two sets of Lewis acid bands whose maxima at 1450 (19b) and 1574 cm^{-1} (8b) shift downward as the evacuation is carried out, at a pressure of 1×10^{-3} Torr. The 19b band, for example, shifts from 1450 in spectrum A to 1445 cm^{-1} in spectrum D (at 523 K). The 8b band at 1574 cm^{-1} shifts to 1556 cm^{-1} at 573 K to give spectrum E. Whereas the 8a band at 1608 cm^{-1} shifts to 1617 cm^{-1} at 623 K, passing by the 1614 cm^{-1} band, shown in spectrum D.

Evacuation at 623 K gives spectrum F which contains a little scope for both 1450 and 1487 cm^{-1} bands with a significant presence for the 1608 cm^{-1} band which shifted to 1617 cm^{-1}.

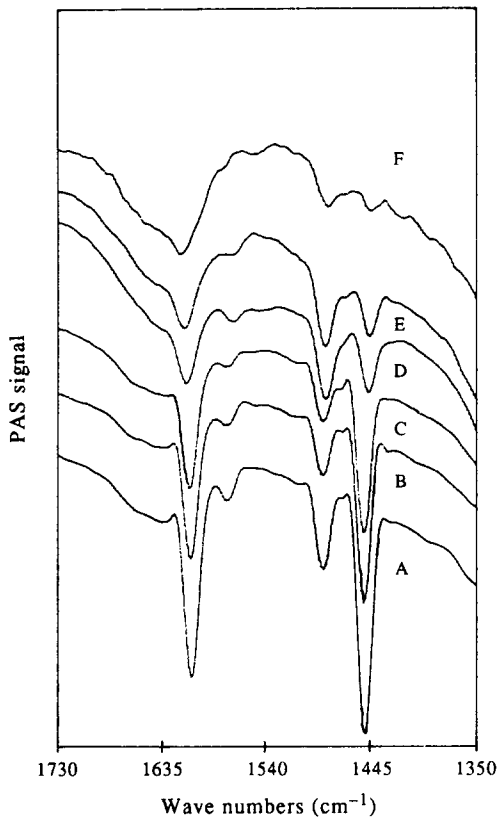

Fig. 3. FTIR/PA spectra of pyridine desorbed from silica gel60 containing the 9wt% CuO–9wt% MoO_3 catalyst, in the 1730–1350 cm^{-1} range, at the following temperatures: (A) 373 K; (B) 413 K; (C) 453 K; (D) 513 K; (E) 573 K; (F) 623 K.

The disappearance of the 8a band at 1636 cm^{-1} is observed at 453 K. The frequencies of both 19b and 8a bands in spectrum F, evacuated at 623 K, reflect the strength of these two sites compared with the rest.

The 8a band which shows a shift in an abrupt manner from 1608 to 1614 and 1617 cm^{-1}, upon evacuation, can be assigned to the presence of three distinct types of coordinatively unsaturated cations.

By comparing the integrated values of the 1450 cm^{-1} peaks vs. the integrated values of the 1487 and 1537 cm^{-1} peaks, as a function of increasing the wt% of copper in the supported catalysts (Table 2), one notices that the intensity of the 1487 cm^{-1} peak is reduced and disappears, reflecting the diminishing of the Bronsted acidity as a result of increasing the copper content.

Table 1. Infrared frequencies of pyridine desorbed from the 9wt% Cu–9wt% Mo/SiO_2 catalyst as a function of evacuation temperatures, shown in Fig. 3

			Evacuation temperature (K), pressure (1×10^{-3}) (Torr)					
			A	B	C	D	E	F
Sample	Type	Mode	373	413	453	523	573	623
9wt%	LPY	19b	1450	1450	1450	1445	1445	1444
Cu–			1465 sh	1465	1465	1465	1465	—
9wt%		19a	1487	1487	1487	1485	1485	1485
Mo/SiO_2		8b	1574	1568	1568	1560	1556	—
		8a	1608	1608	1614	1614	1617	1617
	BPY	19a	1487	1487	1487	1485	1485	1485
		8a	1636	1636	1636	—	—	—

Table 2. Integrated band intensities for the bands near 1450, 1537 and 1487 cm^{-1}, as a function of increasing the copper loading in the following catalysts. This information is deduced from Fig. 1

Samples	Area under the peaks (cm^{-1}) 1537	1450	1487
1wt% Cu–9wt% Mo	0.50	1.13	0.72
3wt% Cu–9wt% Mo	0.08	1.12	0.40
6.6wt% Cu–9wt% Mo	—	1.31	0.43
15wt% Cu–9wt% Mo	—	1.17	0.23

The prominent existence of the band at 1574 cm^{-1} after evacuation at 573 K confirms that this band is not a result of a physisorption interaction. This fact suggests that the 1574 cm^{-1} band can be assigned to pyridine adsorbed on a Lewis acid site. This assignment is supported by the work of CONNELL and DUMESIC [18], who observed a band at 1577 cm^{-1} for Mo–alumina samples.

The large band near 1636 cm^{-1} in spectra D, E and F (Fig. 3) reflects the disappearance of the Bronsted acid site with heating the samples to higher temperatures and most probably Lewis acidity takes over the Bronsted one. Furthermore, such behaviour is only seen for Cu–Mo samples but not for the Mo/SiO_2 sample. Therefore, it is associated only with the presence of copper.

Another report on the MoO_3–SiO_2 catalyst indicated the presence of Lewis acidity and decrease that of Bronsted one rapidly by heat treatment due to Mo ion enhancement [19]. Indeed, this seems acceptable also because the hydrogen-bonded Py is forbidden since it used to have peaks around 1450–1600 cm^{-1}.

Typical half-widths, which are shown in Fig. 1, can be connected to homogeneity of the copper particle sizes on the molybdenum catalyst. Although the CuO/SiO_2 catalyst usually shows a heterogeneous behaviour [20].

Generation of Lewis acid sites and detachment of Bronsted ones

The validity of the TANABE hypothesis [21] cannot be applicable for these catalysts since it is only applied on mixed oxides and not for supported oxides.

Similarly, on applying the SEIYAMA [22] model, who assumes that acidity appears at the boundary where two oxides contact, e.g. on CuO–SiO_2 oxide, indicates a value of $-1/2$ which gives further support to the generation of the Bronsted acidity.

The above failure in predicting the Lewis acid sites involved on the above catalysts, indicates that electronegativity can control the existence of that site on the supported oxides.

The electronegativity of molybdena (3.89) is lower than that of silica (4.14) and the coordination of molybdenum cations is six. However, the coordination of the oxygen anions in molybdena (i.e. 3) is higher than that of silica (i.e. 2), imposing a good chance of forming unsaturated cations, which are responsible for the existence of Lewis acid sites on the silica substrate.

The XRD pattern and UV–vis spectra of the 6.2wt% catalyst shows that most Mo^{6+} are octahedrally coordinated and a MoO_3 phase is formed [23]. The change in site preference from tetrahedral to octahedral Mo coordination above 7wt% MoO_3/Al_2O_3 is also reported using ion scattering spectroscopy [24].

Generally, there is a linear increase of octahedrally coordinated Mo^{6+} as a result of increasing the Mo loading.

Silica does not impart appreciable Lewis acidity due to the absence of coordinatively unsaturated metal cations on the surface.

Introducing the copper ions, in a successive way, forces the Bronsted acidity off and stabilizes that of Lewis ones and induces new forms on the molybdenum–silica catalyst such as CuO and $CuMoO_4$ species.

This is the same as cobalt which acquired a tetrahedral oxygen environment in the $Co–Mo–Al_2O_3$ [25] system. The above result is in agreement with the findings of JEZIOROWSKI *et al.* [9] who reported the detachment of Mo species from the support and the preferential formation of $CoMoO_4$ species is detected.

More evidence for the prevalence of Lewis acidity compared with Bronsted acidity can be obtained by noticing the significant increase of the band at 975 cm^{-1}, which seems to decrease upon increasing the copper loading and is used to measure the polymeric octahedral molybdate species [26], over the tetrahedral species at 950 cm^{-1}, which is indicative for highly dispersed species [23].

As a result of increasing the copper content on the $Cu–Mo/SiO_2$ catalysts, a distortion in the molybdenum structure must be assumed. This also can be confirmed from the 950/975 cm^{-1} ratio, which reflects the possible transformation of octahedral to tetrahedral configuration. According to this hypothesis, $CuO–MoO_3–SiO_2$ should show Lewis acidity expressed in the tetrahedral form.

This result is contrary to that reported by CONNELL and DUMESIC [27] who stated that the cationic Bronsted acid site must be incorporated into the tetrahedral structure of silica. This model explains only the simple cationic Bronsted sites such as Sc^{3+}, Al^{3+} and Ga^{3+}. Concerning the validity of this rule, B^{3+} atom, which can bond tetrahedrally in SiO_2, imparts Lewis acidity and not Bronsted acidity. The same result can be obtained for a copper–silica sample and this reflects the non-applicability of that rule on the supported oxides.

Generally, the difference in electronegativity for Cu^{2+} (1.9) and Mo^{6+} (3.89) doped on silica, of different electronic configuration and different sizes, will probably direct the copper atoms to migrate freely onto the molybdena silica surface. The average electronegativity of molybdenum will become lower and consequently a strong Lewis acidity can be obtained.

Adsorption of carbon monoxide

Metal carbonyl complexes, which are already known in the field of coordination chemistry, are frequently used in various surface adsorption systems.

IR spectra recorded after carbon monoxide adsorption on 9wt% Mo/SiO_2, 9wt% Cu/SiO_2 and 9wt%Cu–9wt%Mo/SiO_2 catalysts are shown in Fig. 4.

The 9wt% Cu sample shows one major band at 2128 cm^{-1} and a very broad band at 2248 cm^{-1}. The former frequency observed during the present study is significantly lower than those observed on high weight percent Cu catalysts (2139 cm^{-1}) [28]. It appears then that the 2128 cm^{-1} band, observed in this investigation, is a result of a fairly high dispersed copper species on the silica catalyst and is assigned to the adsorption of CO on the surface of small CuO particles.

The broad band at 2248 cm^{-1} can be attributed to CO adsorbed on the agglomerated copper clusters, however, an upward shift is observed upon increasing the copper content.

This assignment is a result of the dehydration step (dehydroxylation) obtained for the parent silica followed by copper addition (impregnation method), however, exhibiting a site heterogeneity on the silica support is enhanced.

This confirms that the probability of clustering formation, under this specific condition, is more favourable than the formation of isolated ions, taking into account the high wt% of copper and the weak interaction on the silica surface.

Furthermore, the rather hypsochromic shift of the 2248 cm^{-1} band, if compared with CO adsorbed on supported nickel oxide [29], cobalt oxide [30] and Cu/SiO_2 [31] (prepared by ion exchange), assigned to CO adsorbed on isolated metal surface sites, of a wavelength around 2200 cm^{-1}, is very high.

The 9wt% Mo/SiO_2 spectrum shows a strong band at 2260 cm^{-1} and another strong band at <2100 cm^{-1} with a small shoulder at 2232 cm^{-1}. Small bands are observed at

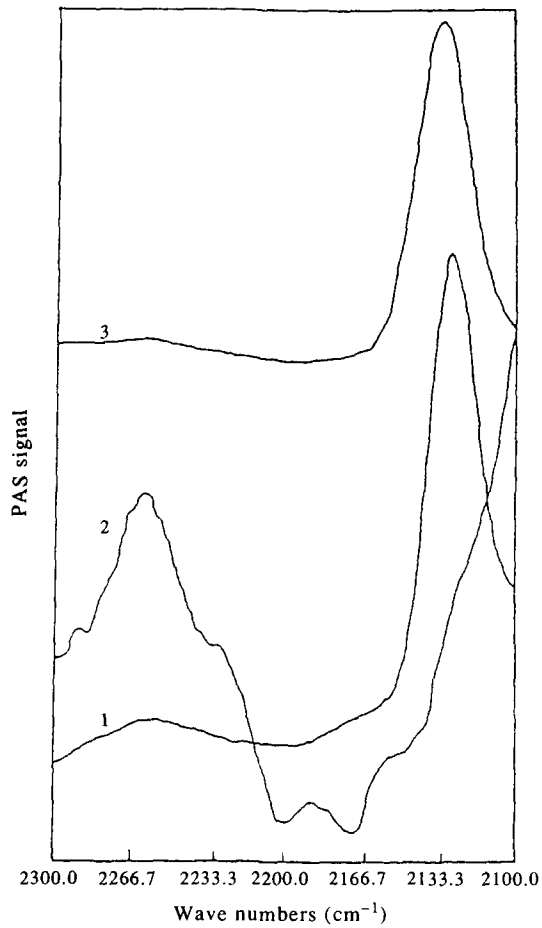

Fig. 4. FTIR/PA spectra of carbon monoxide adsorption on the following precalcined catalysts: (1) 9wt% Cu/SiO; (2) 9wt% Mo/SiO_2; (3) 9wt% Cu–9wt% Mo/SiO_2. All the CO spectra are taken at room temperature.

2185 and 2290 cm^{-1}. This complicated spectrum reflects the expected interaction of CO with Mo, to form bulk carbonyls.

However, the weak interaction of Mo^{6+} with silica favours surface polymerization of Mo species on silica giving rise to a phase which can be reduced below Mo^{6+}. The band at 2260 cm^{-1} can be assigned to CO adsorbed on Mo^{6+}. This assignment is a result of the identification of different phases of high wt% Mo on silica which has been confirmed by many authors. These phases are polymeric molybdate, MoO_3 and Mo–O–Si species [32]. At high Mo loading condensation of MoO_4^{2-} species [26] takes place and according to the weak links between Mo and the SiO_2 support Mo^{6+} ions tend to form free MoO_3 species which are less shielded and more energetic [33] at such high wt% of Mo.

Therefore, the highly energetic polymeric Mo species, which are more versatile ions with various configurations with tetrahedral and octahedral symmetry can be obtained, will be highly favoured than the monomeric species (MoO_4^{2-}---$Mo_7O_{24}^{6-}$) which undergoes a condensation according to the above-mentioned experimental conditions.

The 2232 cm^{-1} band is attributed to the interaction of CO with Mo^{5+}. The strong band at <2100 cm^{-1} is attributed to the adsorption of CO on metallic Mo sites, where the attachment is in linear form and the Mo atoms are in a more reduced environment. Similar assignments are made by others [34, 35], and this result also reflects the extremely high Mo dispersion on the silica support.

The small bands at 2185 and 2290 cm^{-1} can be attributed to CO adsorbed on non-reduced or partially reduced Mo ions but a strict assignment of CO on a definite oxidation state for Mo atoms is less certain.

In the case of a 9wt% Cu–9wt% Mo/SiO_2 sample, a major band at 2133 cm^{-1} and broad band centred around 2236 cm^{-1} are observed.

The bands at 2133 and 2263 cm^{-1} may be compared with maxima at 2128 and 2260 cm^{-1} which have been attributed to CO adsorbed on CuO and on Mo^{6+}, respectively.

The 9wt% Cu–9wt% Mo spectrum is very similar to the 9wt% Cu one, indicating that the surface of the supported oxide is strongly enriched in copper. The continuous disappearance of the 2260 cm^{-1} band in the 9wt% Mo sample reflects the appreciable presence of CuO aggregation which may be superimposed on MoO_3 on the silica surface.

The shifts of CO–Cu and CO–Mo bands from 2128 to 2133 and from 2260 to 2263 cm^{-1}, respectively, reflect the dispersion of the supported oxide compared with the supported individual oxide species.

Acknowledgements—The author is grateful to Professor E. F. Vanant, University of Antwerp, Belgium, for allowing the IR measurements to be carried out in his laboratories.

References

[1] H. Topsoe and B. S. Clausen, *Catal. Rev. Sci. Engng* **26**, 395 (1984).
[2] P. Gajardo, A. Mathieus, P. Grange and B. Delmon, *Appl. Catal.* **3**, 347 (1982).
[3] P. Grange, *Catal. Rev. Sci. Engng* **21**, 135 (1980).
[4] B. Delmon and P. Grange, *Progress in Catalyst Deactivation* (Edited by J. L. Figuereido), p. 231. Nijhoff, The Hague (1982).
[5] B. S. Parekh and S. W. Weller, *J. Catal.* **5**, 58 (1978).
[6] L. C. Tejuca, C. H. Rochester, A. L. Agudo and J. L. G. Firro, *J. Chem. Soc. Faraday Trans. 1* **79**, 2543 (1983).
[7] M. Mokhtar M., C. Vanhoof and E. F. Vansant, *Proc. Int. Symp. on Fourier Transform Spectroscopy*, Antwerp, Belgium, p. 361 (1990).
[8] T. G. Alkhazov, K. U. Adzamov and A. K. Khanmamedova, Oxidative dehydrogenation of butene: scientific research work laboratory of heterogeneous catalysis of oxidation of hydrocarbons, Azizbekov Institute of Petroleum and Chemistry, Baku, USSR (1975).
[9] H. Jeziorowski, H. Knozinger, P. Grange and P. Gajardo, *J. Phys. Chem.* **84**, 1825 (1980).
[10] E. F. Vansant and R. Voets, *J. Chem. Soc. Faraday. Trans 1* **77**, 1371 (1981).
[11] W. Suarz Hill, J. A. Dumesic and G. H. Charles Jr, *J. Catal.* **94**, 408 (1985).
[12] M. Mokhtar M. and E. F. Vansant, *J. Mater. Sci.* submitted for publication.
[13] L. H. Little, *Infrared Spectra of Adsorbed Species*. Academic Press, New York (1966).
[14] K. Tanabe, *Catalysis, Science and Technology* (Edited by J. R. Anderson and M. Bondart), Vol. 2. Springer, New York (1981).
[15] J. B. Goodenough, *4th Int. Conf. on the Chemistry and Uses of Molybdenum* (Edited by H. F. Barry and P. C. H. Mitchell), p. 1. Climax, Ann Arbor, Michigan (1982).
[16] J. Ziolkowski, *J. Catal.* **84**, 317 (1983).
[17] T. Kataoka and J. A. Dumesic, *J. Catal.* **112**, 66 (1988).
[18] G. Connell and J. A. Dumesic, *J. Catal.* **102**, 216 (1986).
[19] T. Komoya, J. Take and Y. Yoneda, *Prepr. 48th Symp. Catal. Catal. Soc. Jpn* 2W16 (1981).
[20] M. A. Kohler, H. E. Curry-Hyde, A. E. Hughes, B. A. Sexton and N. W. Cant, *J. Catal.* **108**, 323 (1987).
[21] K. Tanabe, T. Sumiyoshi, K. Shibata, T. Kiiyoura and J. Kitagawa, *Bull. Chem. Soc. Jpn* **47**, 1064 (1974).
[22] T. Seiyama, *Metal Oxides and their Catalytic Actions*. Kodansha, Tokyo (1978).
[23] S. R. Seyedmonir and F. R. Howe, *J. Catal.* **110**, 216 (1988).
[24] L. Rodrigo, K. Marcinkowska, A. Adont, P. C. Roberge, S. Kaliaguine, J. M. Stencel, L. E. Makovsky and J. R. Diehl, *J. Phys. Chem.* **90**, 2690 (1989).
[25] P. Dufresne, E. Payen, J. Grimblot and J. P. Bonnelle, *J. Phys. Chem.* **85**, 2344 (1981).
[26] T. Liu, M. Forissier, G. Coudurier and J. C. Vedrine, *J. Chem. Soc. Faraday. Trans 1* **85**, 1607 (1989).
[27] G. Connell and J. A. Dumesic, *J. Catal.* **105**, 285 (1987).
[28] K. P. De Jong, J. W. Geus and J. Joziasse, *Appl. Surf. Sci.* **6**, 273 (1980).
[29] J. B. Peri, *Discuss. Faraday Soc.* **41**, 121 (1966).
[30] P. Ratnasamy and H. Knozinger, *J. Catal.* **54**, 155 (1978).
[31] M. A. Kohler, N. W. Cant, M. S. Wainwright and D. L. Trimm, *J. Catal.* **177**, 188 (1989).
[32] H. Jeziorowski and H. Knozinger, *J. Phys. Chem.* **83**(9), 1166 (1979).
[33] P. Gajardo, D. Pirotte, P. Grange and B. Delmon, *J. Phys. Chem.* **83**(13), 1780 (1979).
[34] J. B. Peri, *J. Phys. Chem.* **86**, 1615 (1982).
[35] J.-L. G. Fierro, A. L. Agudo, L. G. Tejuca and C. H. Rochester, *J. Chem. Soc. Faraday Trans. 1* **81**, 1203 (1985).